CHAPTER 4
RESULTS AND DISCUSSION

4.1 Characterization of gelatin from nile tilapia skin

4.1.1 Compositions of nile tilapia skin

The compositions of nile tilapia skin before gelatin extraction are shown in Table 4.1. The fish skin contains 67.71% moisture content. Protein is the major composition in the skin (30.61%wb). The lipid and ash contents are 1.06%wb and 2.06%wb, respectively. Kim and Park (2004) reported that moisture, protein, fat and ash contents of Pacific whiting (*Merluccius productus*) skin were 70.5%, 26.1%, 3.1% and 0.1%, respectively. The compositions of the fish skin of the two species were closely similar. In general, fish skin is low in fat and minerals and is high in protein (collagen) content. The chemical composition of the skin varies with age of the animal, its sex, fat level of the animal, and the treatment the skin has received after being removed from the carcass (Ockerman and Hansen, 1988).

Table 4.1 Proximate compositions of skin from nile tilapia (*Oreochromis niloticus*).

Compositions	Content * (% wb)
Moisture	67.71 ± 0.47
Protein	30.61 ± 0.88
Lipid	1.06 ± 0.10
Ash	2.06 ± 0.40

*Average ± SD from three measurements.

4.1.2 Extraction of gelatin from nile tilapia skin

The yield of gelatin obtained from nile tilapia skin is 18.14% on wet weight basis. The gelatin yields have been reported to vary among fish species, mainly due to the differences in collagen content, the compositions of skin as well as the skin matrix (Jongjareonrak *et al.*, 2006). The different yields of skin gelatin have been reported for sole (8.3%), megrim (7.4%), cod (7.2%), hake (6.5%) (Gomez-Guillen *et al.*, 2002), red tilapia (7.8%) and black tilapia (5.4%) (Jamilah and Harvinder, 2002), young Nile perch (12.5%) and adult Nile perch (16%) (Muyonga *et al.*, 2004), sin croaker (14.3%), shortfin scad (7.25%) (Cheow *et al.*, 2006). The yield of gelatin extracted from nile tilapia skin was higher than those reported by Grossman and Bergman (1992) from tilapia spp. (15%). This higher yield could be due to the efficiency of the gelatin production process or due to complete hydrolysis of the collagen during extraction. (Jamilah and Harvinder, 2002; Cheow *et al.*, 2006).

4.1.3 Physical and chemical properties of gelatin from nile tilapia skin

The proximate compositions of nile tilapia skin gelatin are shown in Table 4.2. The extracted gelatin from skin displayed remarkably high in protein (89.42% wb). The gelatin constituted 7.27% wb water followed by 0.37% wb ash and trace amount of fat (0.28% wb). Nile tilapia skin gelatins contained high protein content but low moisture and fat contents, suggesting the efficient removal of water and fat from skin (Jongjareonrak *et al.*, 2006). Moisture is normally between 9 and 13% wb (renge 7-15% wb) and will vary, not only with the extent of drying but also with the humidity of storage and the moisture permeability of the packaging material (Ockerman and Hansen, 1988). Low ash content shows that the extracted gelatin was of high quality. High quality gelatin has an ash content lower than 0.5%. (Ockerman and Hansen, 1988). The ash content of the extracted gelatin was also lower than the recommended maximum of 2.6% (Jones, 1997). Ash level was reported to vary with the type of raw materials, the method of extraction (Ockerman and Hansen, 1988), and the contents of mineral in raw materials (Jongjareonrak *et al.*, 2006).

Table 4.2 Proximate compositions of gelatin from nile tilapia (*Oreochromis niloticus*) skin.

Compositions	Content * (% wb)
Moisture	7.27 ± 0.45
Protein	89.42 ± 1.30
Lipid	0.28 ± 0.07
Ash	0.37 ± 0.11

*Average ± SD from three measurements.

Table 4.3 shows physical and chemical properties of gelatin from nile tilapia skin. Gel strength is the most important physical property of gelatins (Cheow et al, 2006). The gel strength of gelatin from nile tilapia skin was 328.16 g. The gel strength of fish skin gelatin was reported to vary with species. Gel strength of fish skin gelatins was reported for megrim (340 g), cod (70 g), hake (100 g), sole (350 g) (Gomez-Guillen *et al.*, 2002), red tilapia (128 g), black tilapia (180 g), (Jamilah and Harvinder, 2002), tilapta (263 g), (Grossman and Bergman, 1992), young Nile perch (217 g) and adult Nile perch (240 g), (Muyonga, Cole, and Duodu, 2004), sin croaker (124 g), shortfin scad (176.92 g), (Cheow *et al.*, 2006). Differences in gel strength between species are possibly due to the different compositions of amino acid, size of protein chains (Muyonga, Cole, and Duodu, 2004), concentration and molecular weight distribution of gelatin (Ockerman and Hansen, 1988). The gel strength of gelatin may depend on pH. More compact and stiffer gels can be formed by adjusting the pH of the gelatin close to its isoelectric point, where the protein chains are more neutral and thus align closer to each other (Gudmunsson and Hafsteinsson, 1997).

Table 4.3 Physical and chemical properties of gelatin from nile tilapia (*Oreochromis niloticus)* skin.

Physical and chemical property	
Gel strength (g) at gelatin concentration 6.67% (w/v)	328.16 ± 9.02
Viscosity (cP) at gelatin concentration 6.67% (w/v) at 80 s^{-1}	17.79 ± 0.42
Colour	L* 68.68 ± 1.63
	a* 2.16 ± 0.24
	b* 23.81 ± 0.94
pH	5.03 ±0.21

*Average ± SD from three measurements.

The viscosity of gelatin from nile tilapia skin was 17.79 cP which was higher than those reported by Jamilah and Harvinder (2002). The viscosity of gelatin from red tilapia and black tilapia were 3.2 cP and 7.12 cP, respectively (Jamilah and Harvinder, 2002). Viscosity is the second most commercially important physical property of gelatins (Wainewright, 1977). The viscosity of the fish gelatin in this study can be considered to be in the high-range since viscosities for commercial gelatin have been reported to be from 1.5 to 7.0 cP for most gelatins and up to 13.0 cP for specialized ones (Johnston-Banks, 1990). The viscosity of gelatin solutions is partially controlled by molecular weight and polydispersity of gelatin (Sperling, 1985). Most gelatin has the minimum viscosity when the solution pH is in the 6–8 range. The effect of pH on viscosity is minimum at the isoionic point of the solution and maximum at pH 3 and 10.5. (Jamilah and Harvinder, 2002).

The lightness (L*), redness (a*), and yellowness (b*) of gelatin from nile tilapia skin were 68.68, 2.16, and 23.81, respectively. Gelatin from nile tilapia had a slightly bright yellow-brown appearance. The clarity of gelatin can be improved by treating the solution with diatomaceous earth (Johnston-Banks, 1990). The colour of the gelatin depends on raw material. However, it does not influence other functional properties (Ockerman and Hansen, 1988).

The pH of gelatin from nil e tilapia skin was 5.03. These pH was different compared with the pH of the gelatin from tilapia skin (3.77) obtained by Grossman and Bergman (1992). The difference in pH of the gelatin may be due to the type and strength of acid used during the pretreatment process (Jamilah and Harvinder, 2002).

Table 4.4 Amino acid compositions of gelatin from nile tilapia skin and porcine skin (g/100 g protein)

Amino acids	Nile tilapia skin gelatin	Porcine skin gelatin
Alanine	11.89	12.55
Arginine	8.71	7.43
Glutamic acid	8.99	8.46
Glycine	21.18	22.45
Histidine	0.20	0.20
Isoleucine	0.88	1.06
Leucine	2.12	2.32
Lysine	3.02	3.42
Methionine	1.13	0.82
Phenylalanine	1.74	1.66
Cystine	0.24	0.19
Aspartic acid	8.20	7.84
Tyrosine	0.67	0.81
Proline	8.83	9.80
Hydroxyproline	8.70	9.46
Serine	3.96	3.18
Threonine	5.82	5.92
Tryptophan	0.13	0.12
Valine	1.67	1.98
Imino acid (Pro+Hyp)	17.53	19.26

Note:- Both gelatins were determined using the same method.

The amino acid compositions of gelatin from nile tilapia skin and porcine skin are shown in Table 4.4. It was found that the major amino acid component is glycine in both gelatins. Glycine content in gelatin from nile tilapia skin and porcine skin were 21.18 and 22.45, respectively. Glycine represents nearly one-third of the total amino acid and distributed at every third position of collagen molecule. However, glycine was absent in the first 14 or so amino acid residues from the N-terminus and the first 10 or so from the C-terminus (Foegeding *et al.*, 1996). Relatively high contents of alanine, glutamic acid, proline and hydroxyproline in gelatin from nile tilapia skin were observed. Gelatin from nile tilapia skin had slightly lower in imino acids than gelatin from porcine skin. F oegeding *et al.* (1996) reported that fish collagens contain less imino acids content than mammalian collagens. The imino acids content of gelatin influences the functional properties of gelatin. Gelatins with lower amount of imino acids content have a higher critical concentration and lower melting point, compared with those containing higher amount of imino acids (Gilsenan and Ross-Murphy, 2000). The amino acids content was important for the stabilization of collagen structure (Badii and Howell, 2006). The imino acids (proline and hydroxyproline) impart considerable rigidity to the collagen structure. A relatively limited imino acids content results in a less sterically hindered helix and may affect the mechanical properties of the gelatin (Johnston-Banks, 1990; Badii and Howell, 2006).

The amino acid profile obtained was from an acid hydrolysate of gelatin. A proportion of the acidic amino acids occur as the sidechain amides of glutamine and asparagine in collagen. During acid hydrolysis of gelatin, some of the glutamine and asparagine convert to the acidic forms, i.e. glutamic acid and aspartic acid, respectively (Jamilah and Harvinder, 2002).

4.1.4 SDS-polyacrylamide gel electrophoresis patterns of nile tilapia skin gelatin

The gel electrophoresis patterns of nile tilapia skin gelatin in comparison with porcine skin gelatin are shown in Figure 4.1.

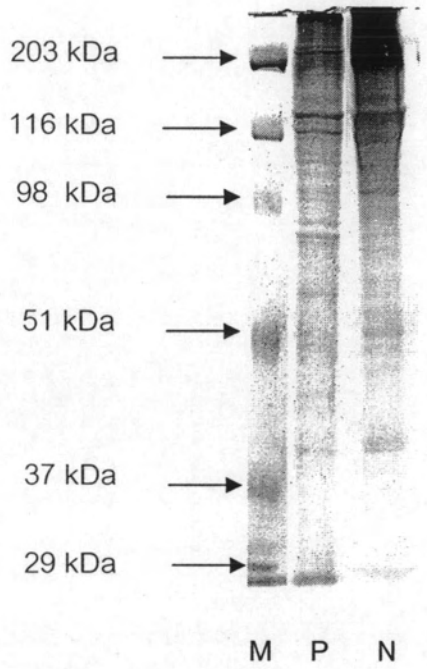

Figure 4.1 SDS-PAGE pattern of nile tilapia skin gelatin and pig skin gelatin. M, P and N denote molecular weight protein markers, porcine skin gelatin and nile tilapia skin gelatin, respectively.

SDS-PAGE pattern of gelatin from nile tilapia skin were similar to gelatin from porcine skin. Nile tilapia skin gelatin consisted of a high proportion of high molecular weight fractions, which are associated with high gelling properties. Low molecular weight fragments were scarcely appreciable in both gelatins. A possible explanation could be that gelatin was not damaged by high temperature and proteinases. Heat activated proteinases, especially collagenase, might involve in the degradation of high molecular weight gelatin. The molecular weight distribution is also important in determining the gelling behavior of gelatin. According to Johnston-Banks (1990), the sum of intact α and β fractions together with their peptides is proportional to the gel

strength while the viscosity, setting rate, and melting point increase with an increase in the amount of high molecular weight (greater than γ) fraction (Muyonga, Cole, and Duodu, 2004).

4.2 Production of nile tilapia skin gelatin nanofiber mat by electrospinning process

4.2.1 Effect of solvent concentration on properties of the fish skin gelain solution and morphological of gelatin nanofibers

The nile tilapia skin gelatin solution properties and the average diameter of the as-spun gelatin nanofibers that had acetic acid as the solvent are shown in Figure 4.2. The applied electrostatic potential used was 15 kV and the distance between tip and ground target was 15 cm. The time of spinning was 10 minutes. According to Figure 4.2, it can be seen that the properties of gelatin solution depend strongly on acetic acid concentration. The viscosity increased and conductivity decreased as acetic acid concentration increased. The viscosity of gelatin solution was found to increase from 345 cP at 10% v/v acetic acid concentration to 1079 cP at 100% v/v acetic acid concentration. When gelatin dissolves in weak acid solution, amino groups binds dissociated hydrions (H^+) causing the chains to carry positive charges and hence repulsion between protein chains. The chains then become extended coils because of the electrostatic action and the viscosity of the solution increases.

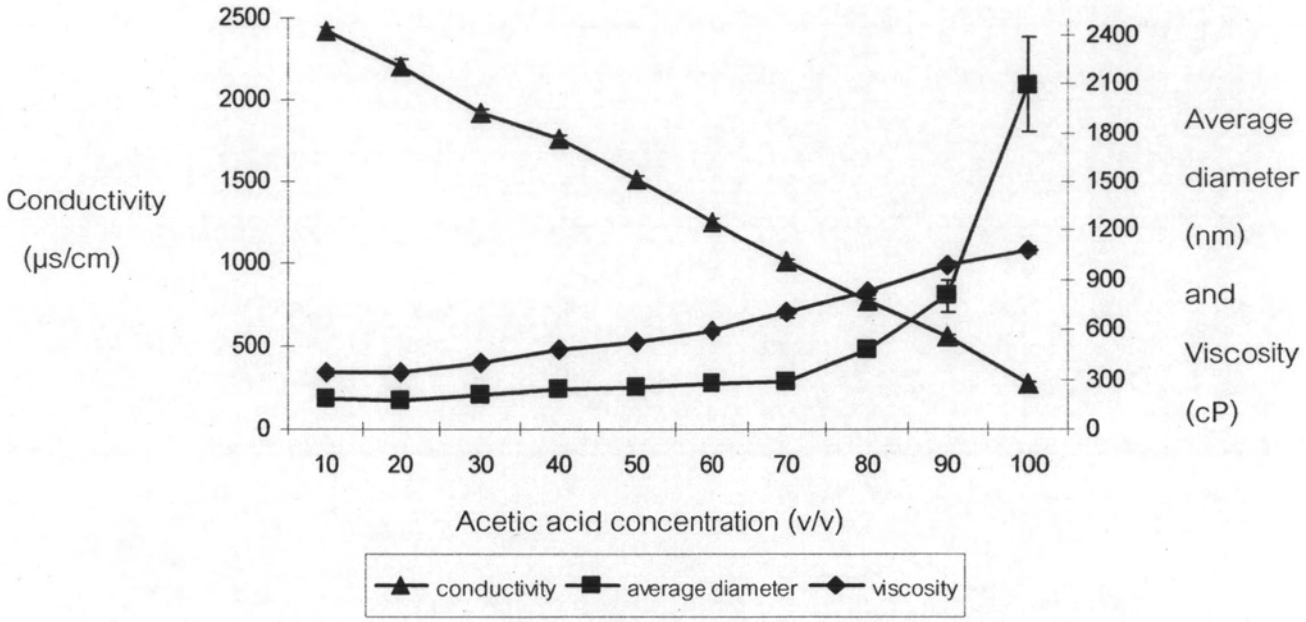

Figure 4.2 The effect of acetic acid concentration on the gelatin solution properties and average gelatin nanofiber diameter.

On the other hand, the conductivity of gelatin solution decreased considerably from 2426 μs/cm at 10% v/v acetic acid concentration to 268 μs/cm at 100% v/v acetic acid concentration. The decrease of conductivity is due to free ions that transport charge decrease when acetic acid concentration increases. The average fiber diameter was found to increase with increasing acetic acid concentration from 179 nm at 10% v/v acetic acid concentration to 2095 nm at 100% v/v acetic acid concentration.

The properties of nile tilapia skin gelatin in 10%-100% v/v formic acid and the average diameter of the as-spun gelatin nanofibers are shown in Figure 4.3. The viscosity of the solution increased with increasing formic acid concentration from 236 cP at 10% v/v formic acid concentration to 939 cP at 100% v/v formic acid concentration. Like the gelatin in acetic acid solution, the conductivity of gelatin solution in formic acid decreased considerably with increasing formic acid concentration from 5587 μs/cm at 10% v/v formic acid concentration to 3103 μs/cm at 100% v/v formic acid concentration. The average fiber diameter was found to increase with increasing formic acid

concentration from 143 nm at 10% v/v formic acid concentration to 225 nm at 100% v/v formic acid concentration.

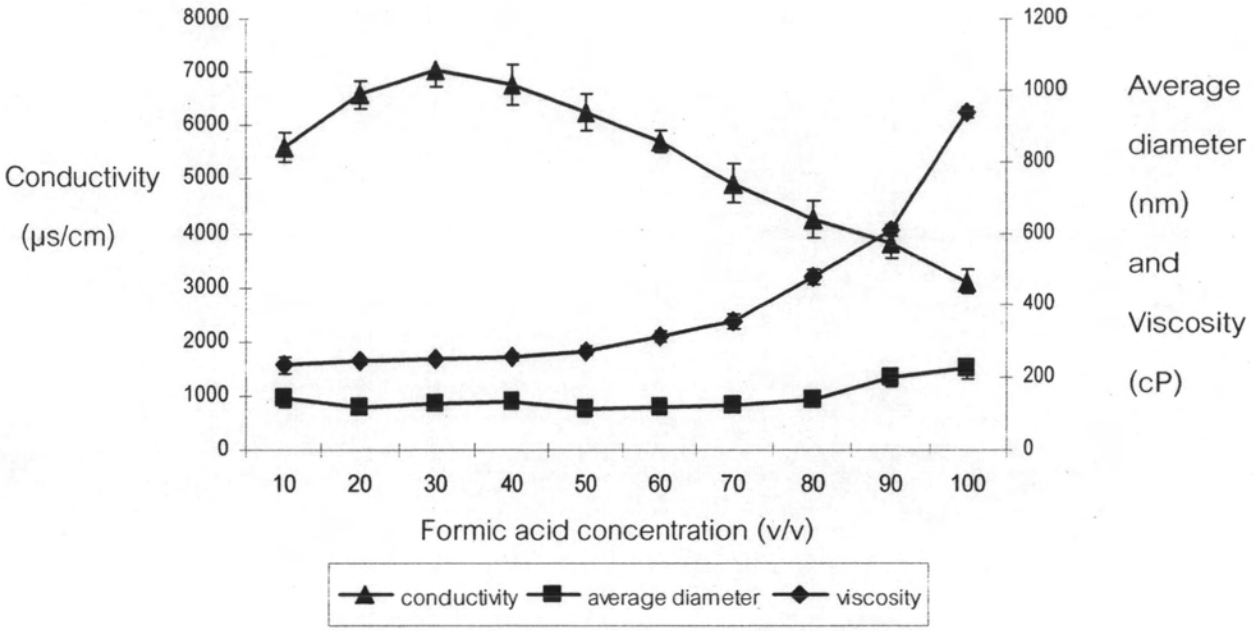

Figure 4.3 The effect of formic acid concentration on the gelatin solution properties and average gelatin nanofiber diameter.

In the present case when the electrospinning was performed at room temperature, the spinning ability depended mainly on the viscosity of solution. Figure 4.4 shows SEM photographs of electrospun gelatin/acetic acid fiber at 15% w/v gelatin concentration and various acetic acid concentrations. Continuous fibers were successfully electrospun from the gelatin solutions in 10%-100% v/v acetic acid solvent. However the acetic acid concentration of 10% and 20% gave bead-on-string nanofibers. The beads disappeared when the acetic acid concentration was between 30%-70% v/v. Figure 4.5 shows SEM photographs of electrospun gelatin/formic acid fiber at 15% w/v gelatin concentration and various formic acid concentrations. With formic acid solvent, continuous fibers were successfully electrospun from the gelatin solutions in 10%-100% v/v formic acid concentrations. But bead-on-string nanofibers occurred at the formic acid concentration between 10%- 70%.

The occurring of beads has been well known being related to the solution viscosity, which is varied with the solution concentration. The presence of beads was due to the low viscosity and high surface tension of the gelatin solution. The occurrence of bead was found to reduce with increasing solution viscosity. Increasing solution viscosity also causes an increase in diameter of the beads and an increase in the average distance between beads on the fibers. Concurrently, the shape of the beads gradually changes from spherical to spindle-like as the solution viscosity increases (Fong, chun and reneker, 1999).

It has been found in this study that the more viscous solution at acetic acid concentration between 80%-100% v/v and formic acid concentration between 90%-100% v/v was more difficult to be processed into nanofibers through the electrospinning technique. The difficulty in electrospinning using high concentration solution was that highly viscous fluid balls would be gradually gathered outside the tip of the needle after the electrospinning had started for a while no matter how high an electric voltage had been applied and hence a few fibers were resulted. Moreover, only a portion of the electrically charged solution jets seemed to have been solidified into ultra fine fibers. The remaining portion must have been still in the fluid form when reaching the target collector (Huang et al, 2004).

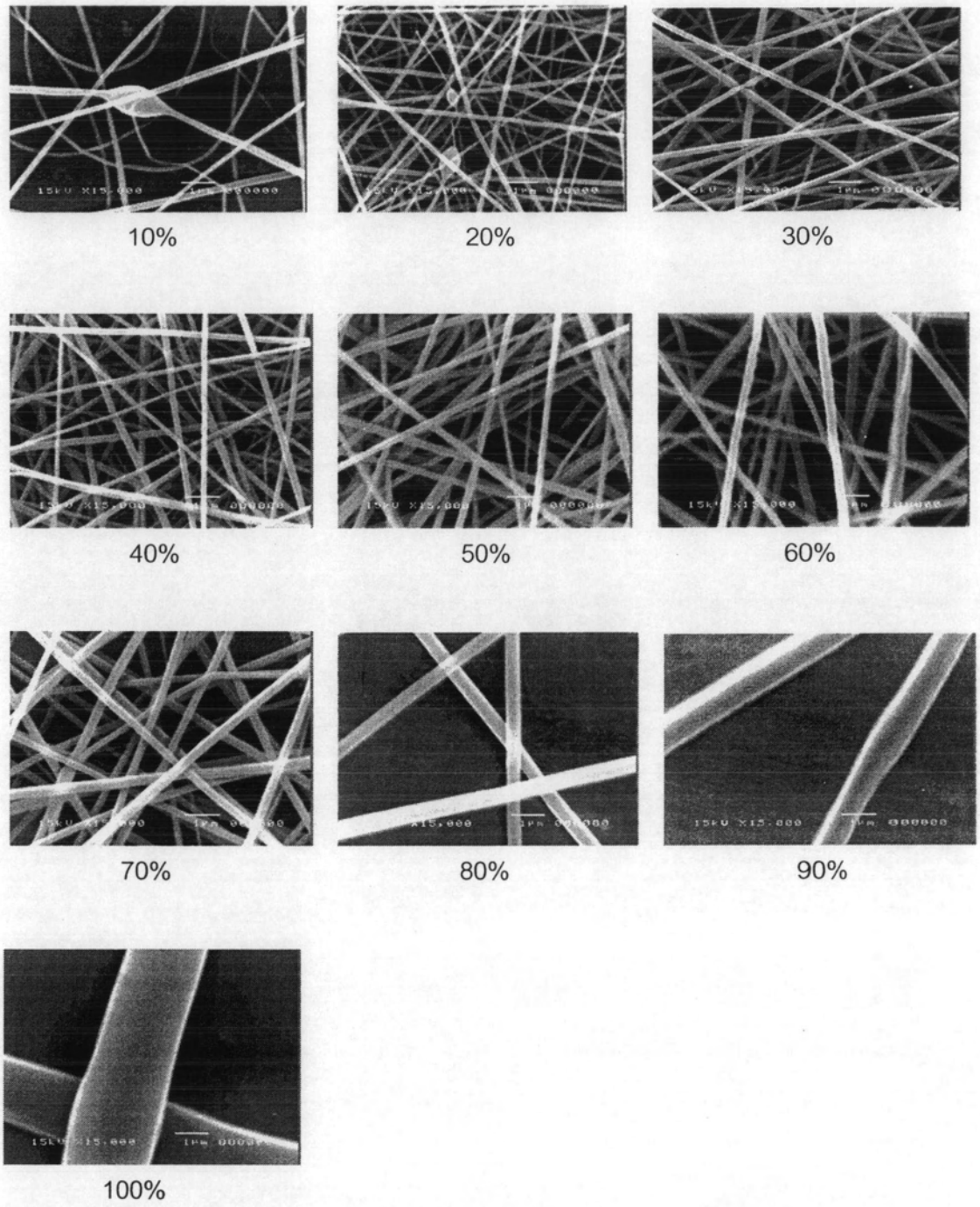

Figure 4.4 SEM photographs of electrospun gelatin/acetic acid fibers at 15% w/v gelatin concentration and various acetic acid concentrations (10%-100% acetic acid concentrations).

Note: All SEM photographs used 15000x magnification and 1 μm scale bar.

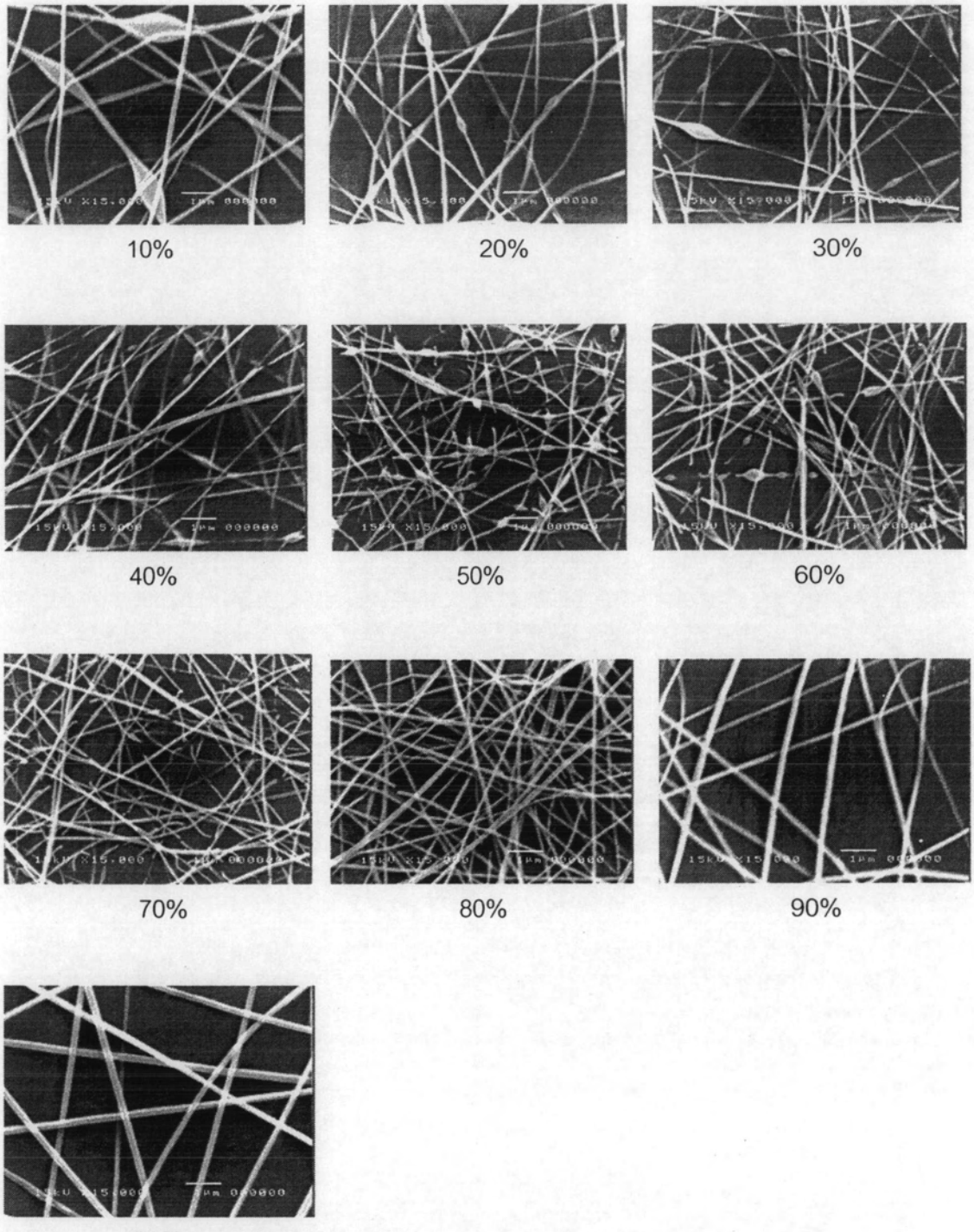

Figure 4.5 SEM photographs of electrospun gelatin/formic acid fibers at 15% w/v gelatin concentration and various formic acid concentrations (10%-100% formic acid concentrations).

Note: All SEM photographs used 15000x magnification and 1 μm scale bar.

In this study, 40% v/v acetic acid concentration was chosen in order to produce ultra fine and bead-free nanofibers mat in the following experiment. At 40% v/v acetic acid concentration, the resulting smooth and uniform ultra fine fibers had a diameter of 233 nm. Although 10%-30% v/v acetic acid concentration gave smaller fiber diameters, beads occurred on the fiber surface at these concentrations. As for formic acid, the concentration of 80% v/v was chosen. At 80% v/v formic acid concentration, the resulting smooth and uniform ultra fine fibers had a diameter of 137 nm. 10%-70% v/v formic acid concentration gave bead-on-string fibers. Although 90%-100% v/v formic acid concentration gave the smooth and uniform fiber, the number of as-spun fibers per unit area was found to decrease.

4.2.2 Effect of gelatin concentration on properties of the fish skin gelatin solution and morphological of gelatin nanofibers

The conductivity and viscosity of 5%-29% w/v gelatin solution in 40% v/v acetic acid and the average diameter of the as-spun gelatin nanofibers are shown in Figure 4.6. According to Figure 4.6, the viscosity, conductivity, and the average nanofiber diameter increased with increasing gelatin concentration. The viscosity of gelatin solution increased from 39 cP at 5% w/v to 4546 cP at 29% w/v. Changes in viscosity could be attributed to increased polymer chain entanglement of gelatin at increasing gelatin concentrations. No entanglement was reported for dilute and semi-dilute dispersions, while entanglement was found in the more concentrated solutions that led to the formation of continuous fibers (Wongsasulak *et al.*, 2006). Gupta *et al.* (2005) also reported that the morphology of electrospun materials is influenced by polymer viscosity.

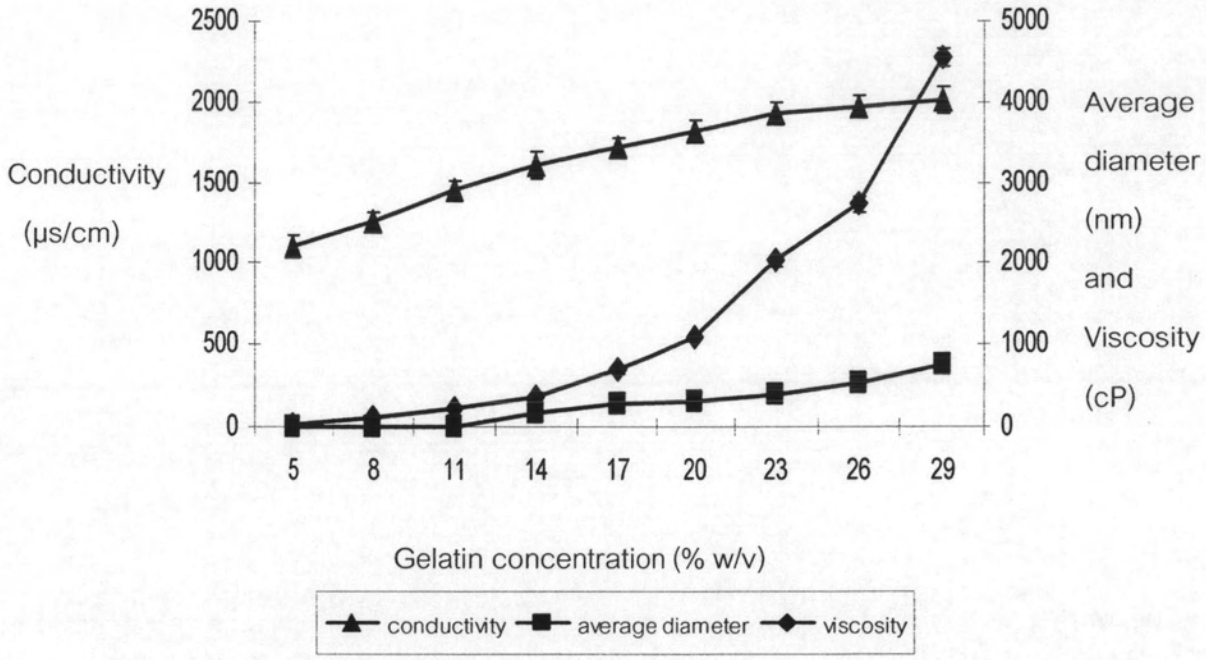

Figure 4.6 The effect of gelatin concentration on the solution properties and average gelatin nanofiber diameter when 40% v/v acetic acid was used as the solvent.

The conductivity of gelatin solution increased from 1108 μs/cm at 5% w/v to 2010 μs/cm at 29% v/v. For acetic acid and formic acid solvents, there were dissociated carboxylic acidic ions ($R\text{-}COO^-$), hydrions (H^+), and undissociated carboxylic acid molecules (R-COOH). When gelatin dissolves in weak acid solutions, amino groups first bind dissociated hydrions. When dissociated hydrions were bound completely, with the increase of gelatin concentration, the excessive gelatin began to interact with undissociated carboxylic acid molecules by which charge were transported. Therefore, the specific conductivity of gelatin solution increased. The average fiber diameter was found to increase with increasing gelatin concentration from 161 nm at 5% w/v to 761 nm at 29% w/v gelatin concentration.

According to Figure 4.7, the viscosity, conductivity and the average nanofiber diameter increased with increasing gelatin concentration. The viscosity of gelatin solution increased from 81 cP at 5% w/v to 3705 cP at 29% w/v. The conductivity of gelatin solution increased from 2070 μs/cm at 5% w/v to 3657 μs/cm at gelatin concentration of 29% v/v. The average nanofiber diameter increased with increasing gelatin concentration from 109 nm at 5% w/v to 302 nm at 29% w/v gelatin concentration.

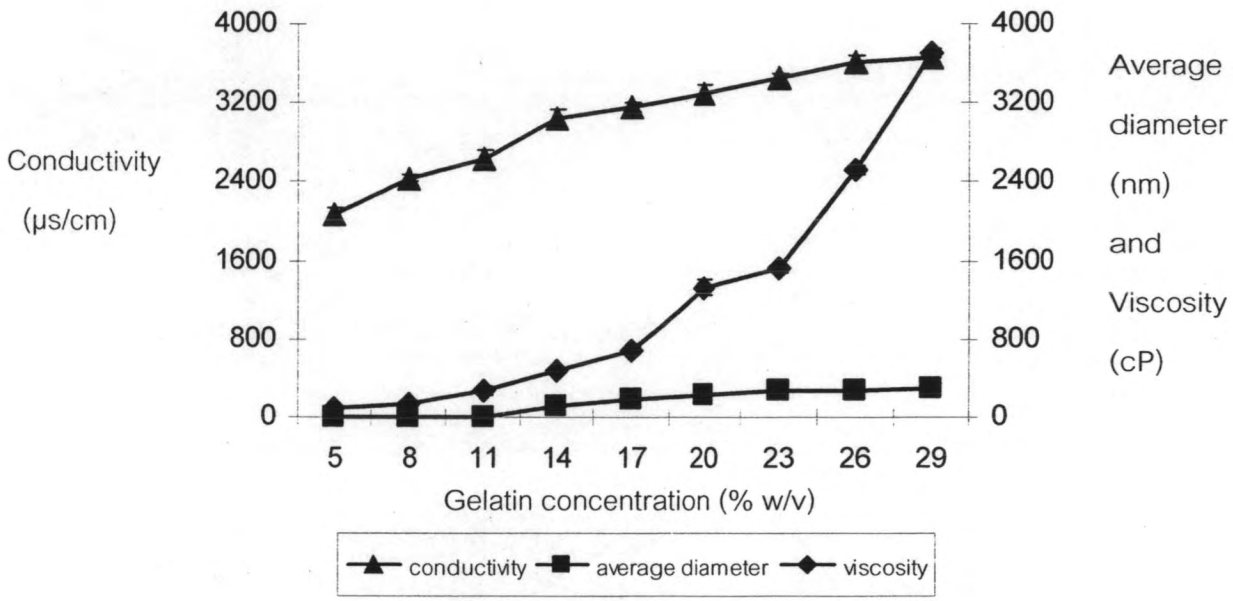

Figure 4.7 The effect of gelatin concentration on the solution properties and average gelatin nanofiber diameter when 80% v/v formic acid was used as the solvent.

Figure 4.8 shows SEM photographs of electrospun gelatin/acetic acid nanofiber at various gelatin concentrations. At low gelatin concentrations (between 5 and 11% w/v), no continuous fiber except for beads and bead assemblages were obtained, although some fiber segments existed. At low concentrations, the viscosity of the gelatin solution was low, while the surface tension was relatively high. Therefore, the solution jet, which would form a nanofiber, could not maintain its own shape at the end

of the syringe tip due to high surface tension and formed small drops among the fibers. This caused the occurrence of beads instead of the formation of nanofiber and thus reduced the uniformity of electrospun gelatin web (Ki *et al.*, 2005). The amount of beads decreased and disappeared altogether when the gelatin concentration increased to a concentration between 17%-29% w/v. The number of as-spun fibers per unit area decreased at high gelatin concentration (29% w/v).

Figure 4.9 shows selected SEM photographs of as-spun gelatin/formic acid nanofiber at various gelatin concentrations. At 5 and 8% w/v concentration, continuous nanofiber could not form. At 11 and 14% w/v gelatin concentration, fiber segment with beads formed. At 17% w/v, the continuous fiber formed but some beads were found. The presence of continuous fiber with no bead was evident when the gelatin concentration was between 20%-29% w/v.

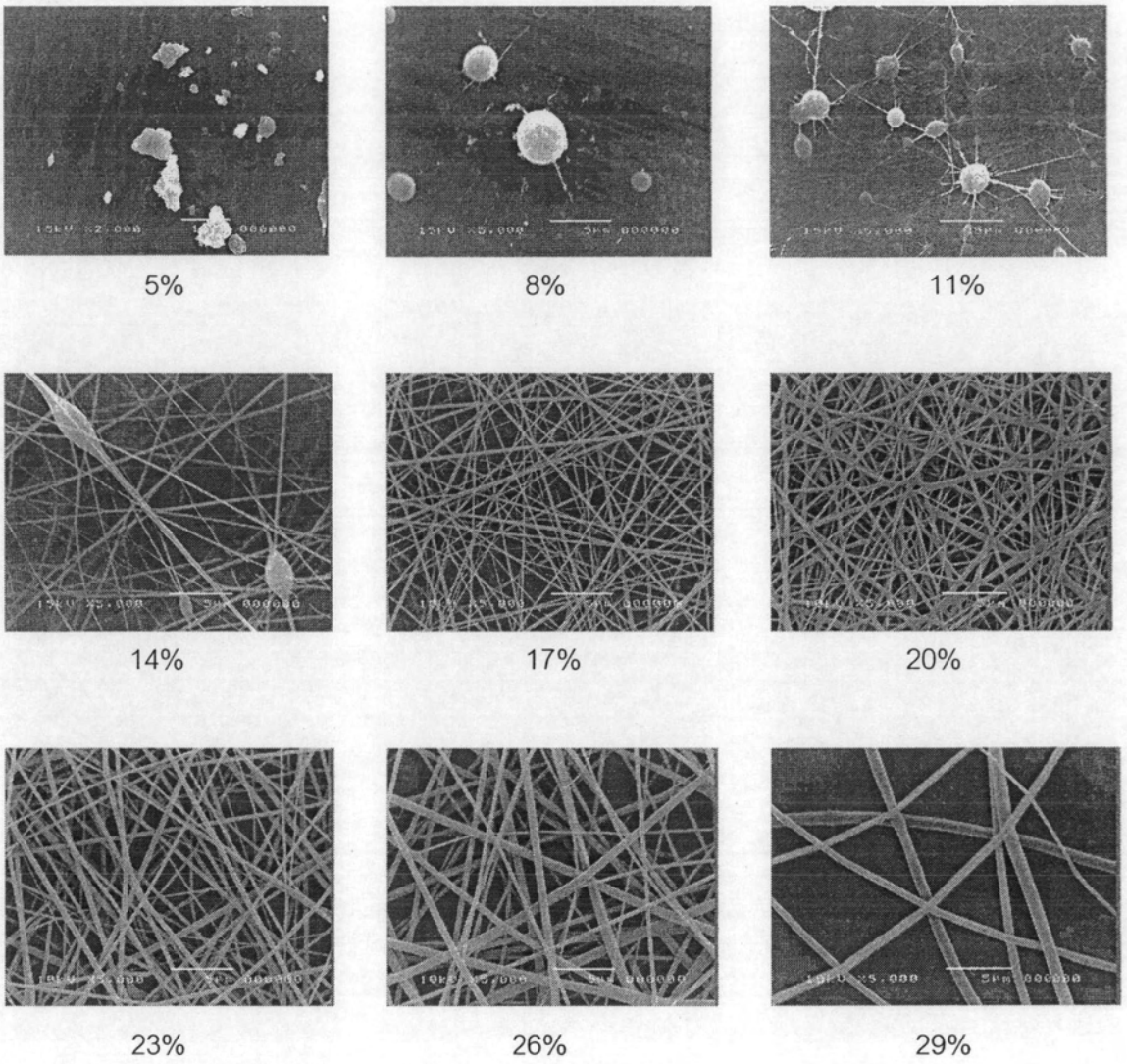

Figure 4.8 SEM photographs of electrospun gelatin/acetic acid nanofibers with varying gelatin concentrations (5% - 29% w/v).

Note: The SEM photograph at 5% w/v gelatin concentration was taken at 2000x magnification and those at 8%-29% w/v gelatin concentration were taken at 5000x magnification.

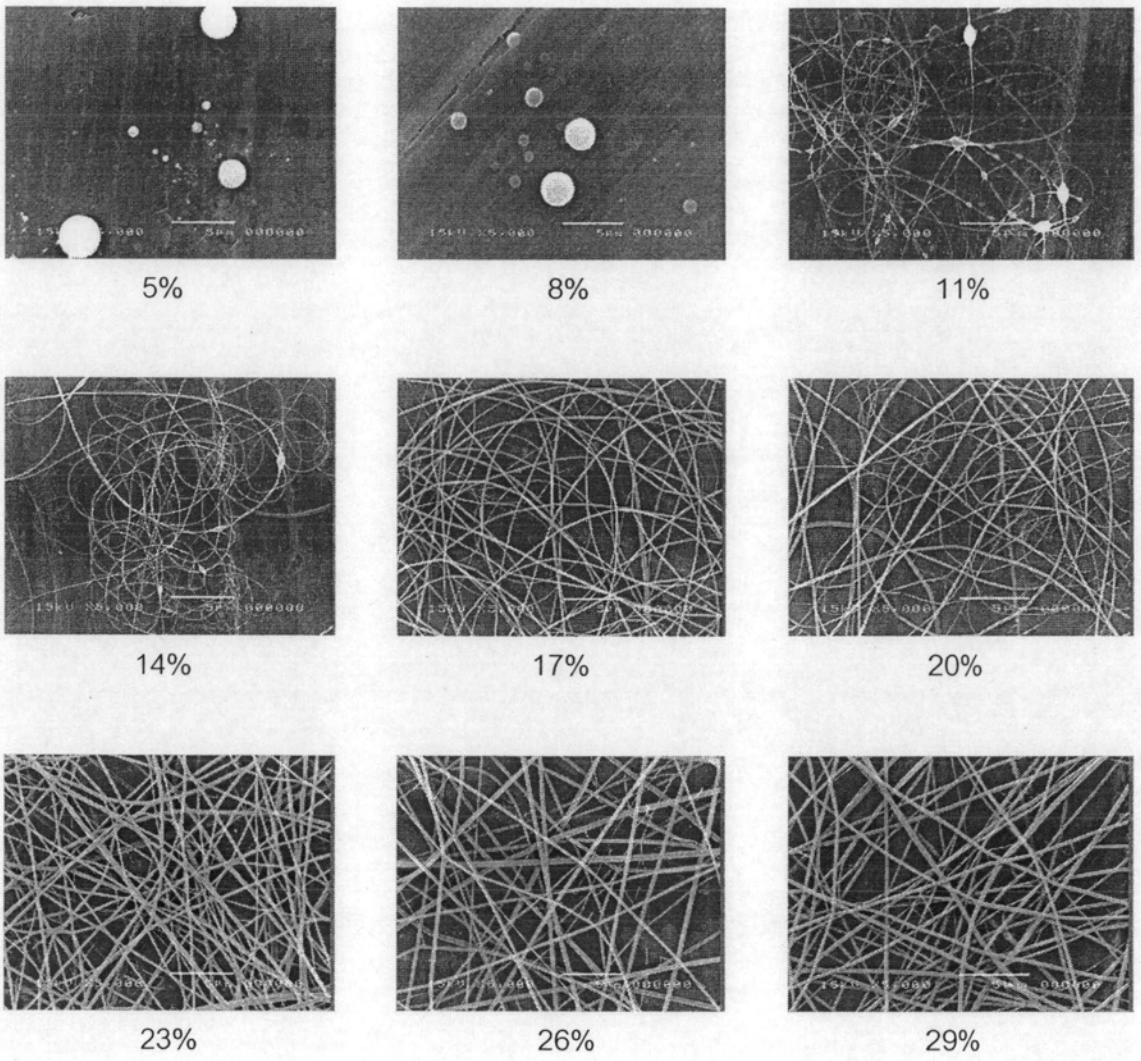

Figure 4.9 SEM photographs of electrospun gelatin/formic acid nanofibers with varying gelatin concentrations (5% - 29%).

Note: All SEM photographs were taken at 5000x magnification.

The gelatin concentration that yielded smooth and uniform fibers were 17, 20 and 23% w/v gelatin in 40% v/v acetic acid solvent system. The average fiber diameters were between 207 nm and 398 nm. In 80% v/v formic acid solvent, 20%-26% w/v gelatin solutions gave smooth and uniform fibers. The average fiber diameters were between 238 nm and 284 nm. These gelatin concentrations were chosen for further study.

Acetic acid and formic acid can be used as gelatin's solvent for electrospinning due to its high volatility. Formic acid has been noted as a good organic solvent for various polypeptide-based polymers. Moreover, the evaporation rate of formic acid in ambient air (22 °C) has been reported to be 2.3 x 10^{-8} g/mm^2/s (Wongsasulak *et al.*, 2006). The difference in electrospinnability between gelatin in acetic acid solution and gelatin in formic acid solution may depend on the solvent properties as shown in Table 4.5. Fiber dimeters decreased with increasing density and boiling point of sovent. Productivity of fibers increased with increasing dielectric constant and dipole moment of the solvents (Wonnatong *et al.*, 2004). Due to higher acid dissociation equilibrium constant (K_a), formic acid has higher conductivity. The high conductivity of formic acid resulted in difficulty in processing nanofibers through electrospinning technique because the charge jets were ejected very fast and reached the target collector before complete solvent evapopation causing beads to form.

Table 4.5 Properties of acetic acid and formic acid.

	Acetic acid	Formic acid
Density (g.cm^{-3})	1.05	1.22
Viscosity (cP)	1.12	1.57
Boiling point (°C)	118	100.8
Dipole moment (D)	1.68	1.41
Dielectric constant	6.15	58
Ka	1.8 x 10^{-5}	1.8 x 10^{-4}

4.2.3 Mechanical properties of gelatin nanofibers mat

Refer to 4.2.1 and 4.2.2, acetic acid and formic acid concentrations and gelatin concentration were selected in order to produce mat formed by continuous bead-free gelatin nanofibers. It was found that the as-electrospun nanofibers structure of gelatin is water soluble and mechanically weak. Crosslinking treatment would be able to improve both water-resistant ability and thermo-mechanical performance of the resulting nanofibers mats (Zhang *et al.*, 2006). Therefore, the gelatin nanofiber mats produced from the selected conditions were crosslinked with glutaraldehyde vapor. The crosslinked gelatin nanofibers mats were to be compared with non-crosslinked gelatin nanofibers mats. The result will be shown later in this section.

Tensile strength, Young's modulus, and elongation of the electrospun gelatin/acetic acid nanofiber mats with 17, 20, and 23% w/v gelatin concentrations before and after crosslinking are shown in Figures 4.10-4.12. The tensile strength of crosslinked gelatin nanofibers mats at all gelatin concentrations was significantly higher ($P \leq 0.05$) than that of the non-crosslinked gelatin fiber mats. Young's modulus of crosslinked gelatin nanofibers mats at 17 and 20% gelatin concentrations was significantly higher ($P \leq 0.05$) than that of the non-crosslinked gelatin fiber mats. Young's modulus of the crosslinked and non-crosslinked gelatin nanofibers mats at 23% gelatin concentrations did not differ significantly ($P > 0.05$). But the elongation of the crosslinked and non-crosslinked gelatin nanofibers mats at all gelatin concentrations did not differ significantly ($P > 0.05$).

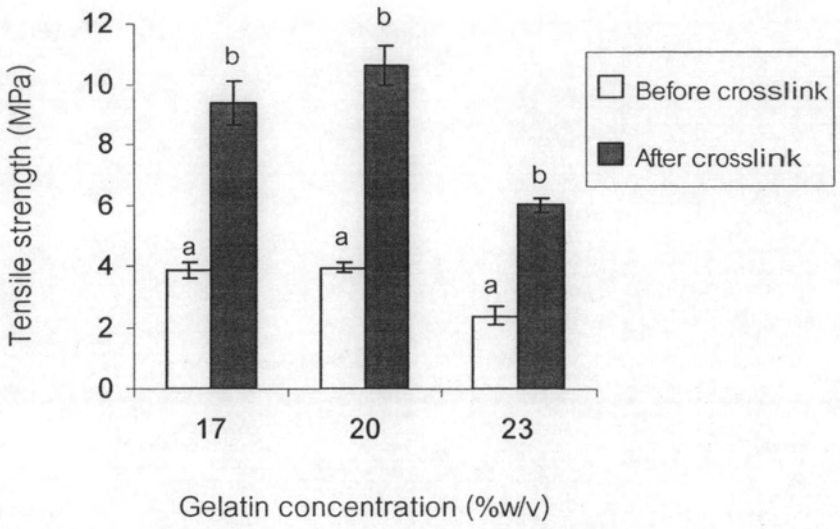

Figure 4.10 Tensile strength of the electrospun gelatin/acetic acid nanofiber mats with 17, 20, and 23% w/v gelatin concentrations before and after crosslinking.

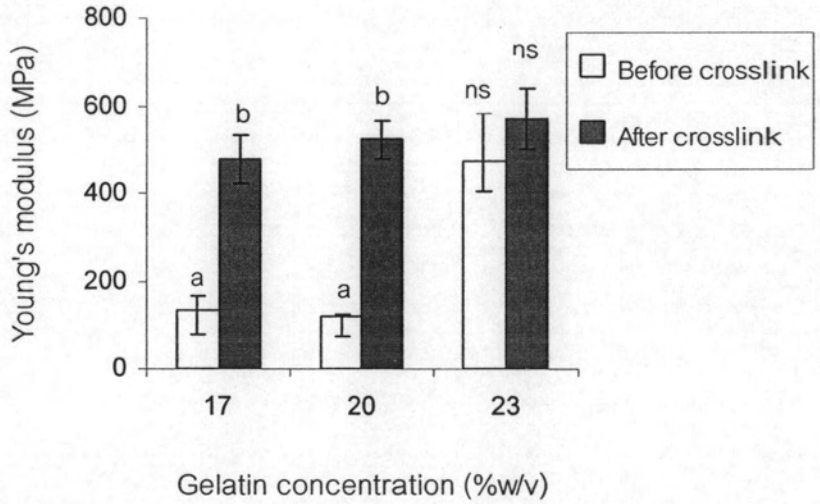

Figure 4.11 The Young's modulus of the electrospun gelatin/acetic acid nanofiber mats with 17, 20, and 23% w/v gelatin concentrations before and after crosslinking.

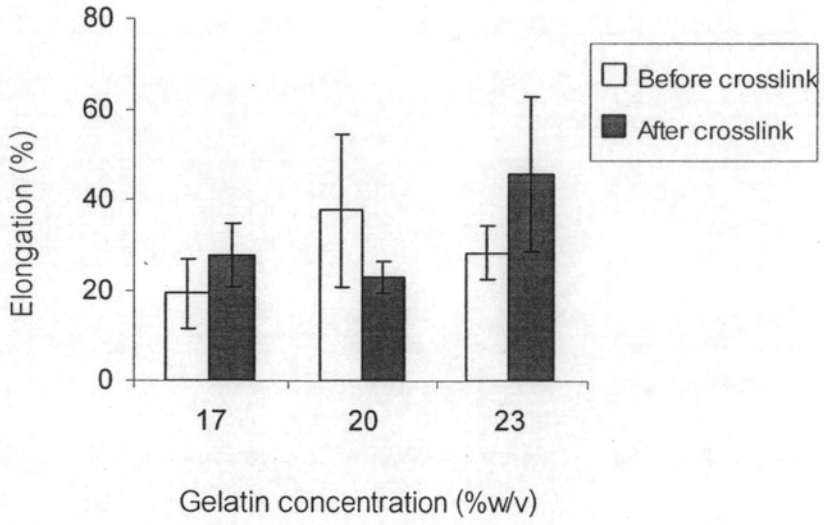

Figure 4.12 Elongation of the electrospun gelatin/acetic acid nanofiber mats with gelatin concentrations at 17, 20, and 23% w/v before and after crosslinking.

Note: All value do not differ significantly ($P > 0.05$).

Tensile strength, Young's modulus and elongation of the electrospun gelatin/formic acid nanofiber mats with 20, 23, and 26% w/v gelatin concentrations before and after the crosslinking are shown in Figures 4.13-4.15. The tensile strength of crosslinked gelatin nanofibers mats at 20 and 26% gelatin concentrations was significantly higher ($P \leq 0.05$) than that of the non-crosslinked gelatin fiber mats. The tensile strength of crosslinked gelatin nanofibers mats at 23% gelatin concentrations did not differ significantly ($P > 0.05$) from non-crosslinked gelatin fiber mats. Young's modulus of crosslinked gelatin nanofibers mats at all gelatin concentrations was significantly higher ($P \leq 0.05$) than that of the non-crosslinked gelatin fiber mats. But the elongation of the crosslinked and non-crosslinked gelatin nanofibers mats at all gelatin concentrations did not differ significantly ($P > 0.05$).

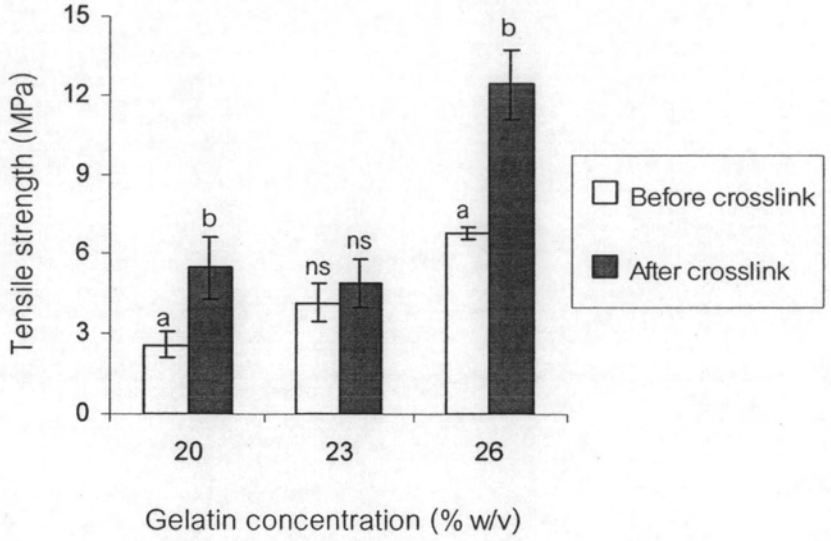

Figure 4.13 Tensile strength of the electrospun gelatin/formic acid nanofiber mats with gelatin concentrations at 20, 23, and 26% w/v before and after crosslinking.

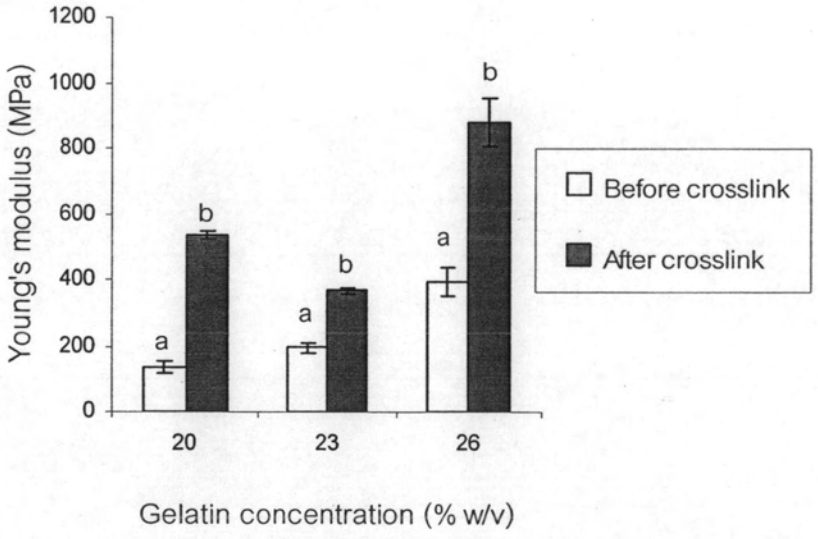

Figure 4.14 The Young's modulus of the electrospun gelatin/formic acid nanofiber mats with gelatin concentrations at 20, 23, and 26% w/v before and after crosslinking.

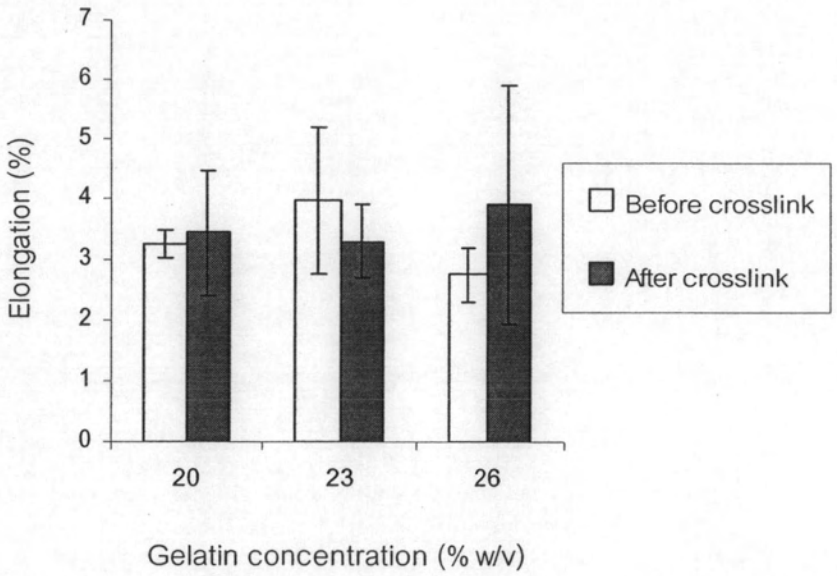

Figure 4.15 Elongation of the electrospun gelatin/formic acid nanofiber mats with gelatin concentrations at 20, 23, and 26% w/v before and after crosslinking.

Note: All value do not differ significantly ($P > 0.05$).

Figures 4.16 and 4.17 show SEM photographs of electrospun gelatin/acetic acid and gelatin/formic acid nanofiber from gelatin solutions before and after crosslinking with glutaraldehyde. It was visible from these photographs that inter- and intra-molecular covalent bonds and the bondings between the fiber junctions were formed. Zhang *et al.* (2006) reported that crosslinking of collagenous materials with glutaraldehyde involves the reaction of free amino groups of lysine or hydroxylysine amino acid residues of the polypeptide chains with the aldehyde groups of glutaraldehyde. This was responsible for the improvement in mechanical properties of gelatin nanofiber mats. Formation of point-bonded structures favors the structural integrity of electrospun fibers, hence, resulting in improved mechanical properties.

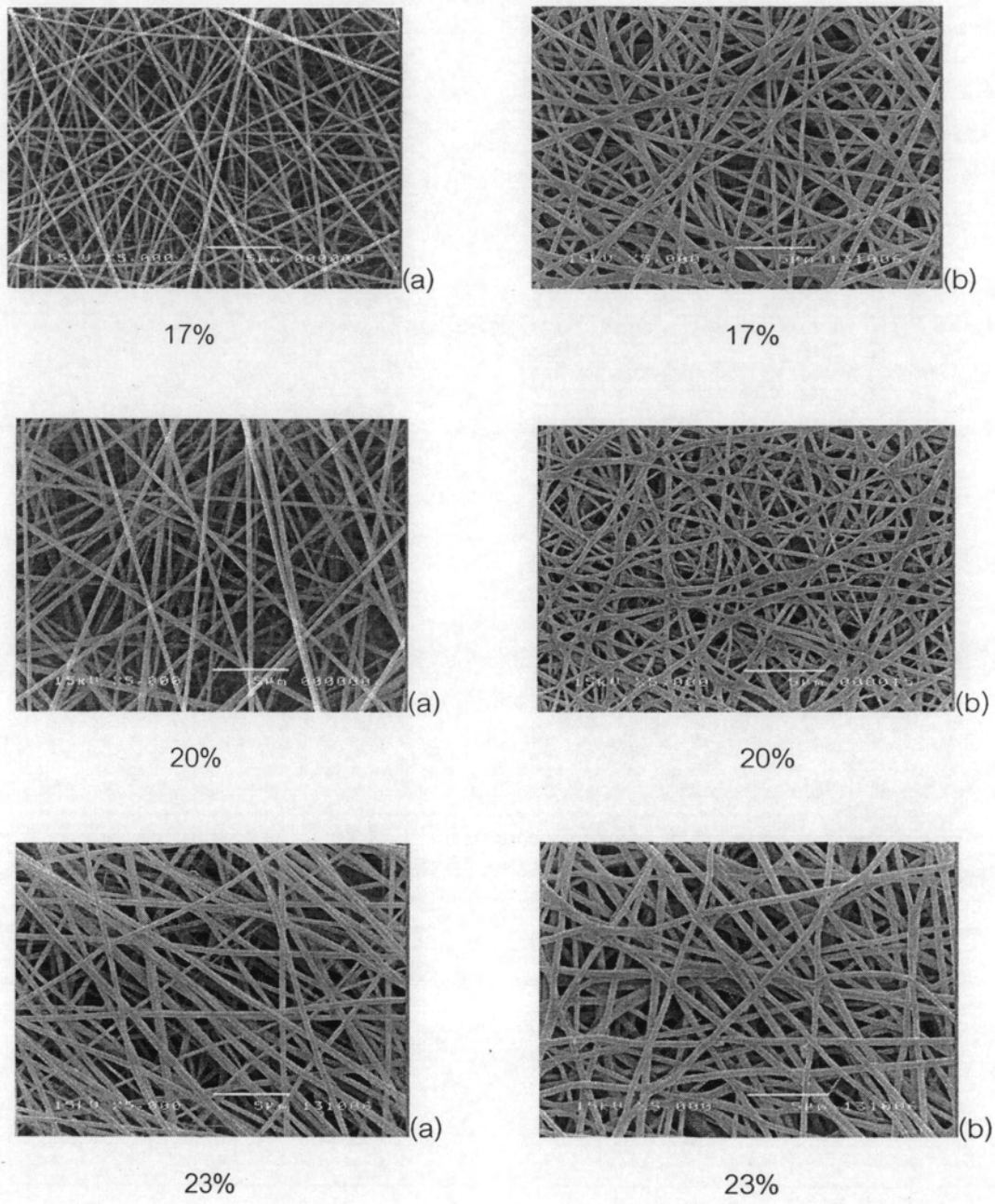

Figure 4.16 SEM photographs of electrospun gelatin/acetic acid nanofibers mats with gelatin concentrations at 17, 20 and 23% w/v; (a) before crosslinking, and (b) after crosslinking.

Note: All SEM photographs were taken at 5000x magnification.

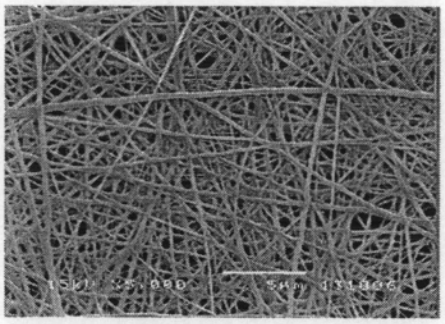
(a)

20%

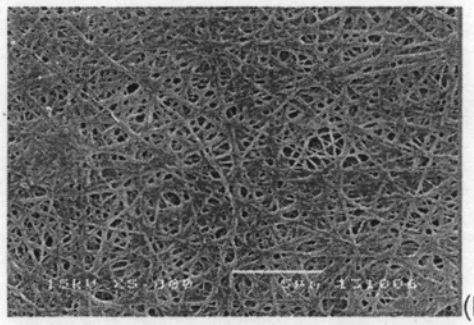
(b)

20%

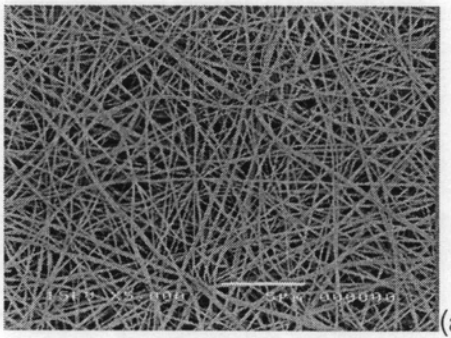
(a)

23%

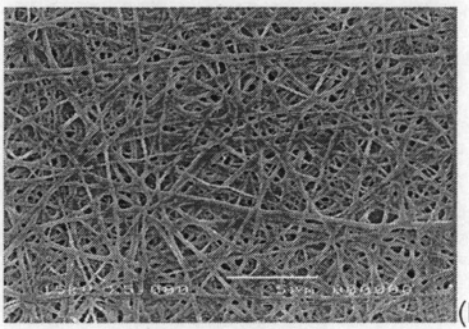
(b)

23%

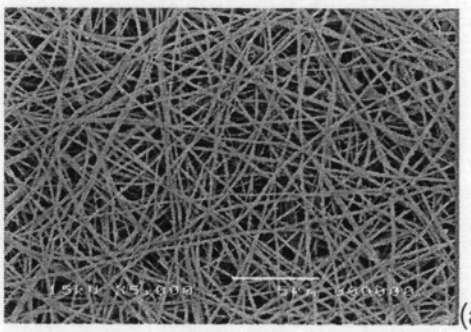
(a)

26%

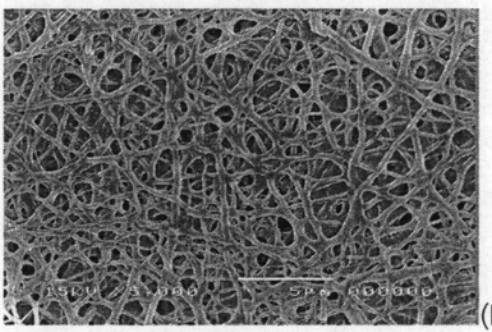
(b)

26%

Figure 4.17 SEM photographs of electrospun gelatin/formic acid nanofibers mats with gelatin concentrations at 20, 23 and 26% w/v; (a) before crosslinking, and (b) after crosslinking.

Note: All SEM photographs were taken at 5000x magnification.

Table 4.6 and 4.7 show lightness (L*), redness (a*), and yellowness (b*) of the electrospun gelatin/acetic acid and gelatin/formic acid nanofiber mats produced from gelatin solution at various concentrations before and after crosslinking. The lightness (L*) and redness (a*) of the non-crosslinked mat produced from both solvent systems were lower when compared with the electrospun nanofiber mat that was crosslinked with glutaraldehyde. However, the yellowness (b*) of the crosslinked electrospun nanofiber was higher when compared with the non-crosslinked gelatin nanofiber mat. The colour of the gelatin nanofiber mat was visibly yellowish and the mat slightly shrunk after crosslinking. The colour change was due to the establishment of aldimine linkages (CH=N) between the free amine groups of protein and glutaraldehyde (Zhang *et al.*, 2006).

Table 4.6 The lightness (L*), redness (a*), and yellowness (b*) of electrospun gelatin/acetic acid nanofiber before and after crosslinking.

Gelatin concentration (% w/v)		Lightness (L*), redness (a*), and yellowness (b*)	
		Before crosslink	After crosslink
17	L*	96.62 ± 0.63	94.80 ± 0.19
	a*	-0.24 ± 0.02	-0.36 ± 0.07
	b*	0.58 ± 0.10	8.45 ± 0.29
20	L*	96.56 ± 1.39	95.43 ± 0.14
	a*	-0.03 ± 0.05	-0.51 ± 0.09
	b	0.22 ± 0.23	7.65 ± 0.24
23	L*	97.89 ± 0.32	95.18 ± 0.15
	a*	0.18 ± 0.04	0.05 ± 0.03
	b	0.61 ± 0.03	7.95 ± 0.09

Table 4.7 The lightness (L*), redness (a*), and yellowness (b*) of electrospun gelatin/formic acid nanofiber mats before and after crosslinking.

Gelatin concentration (% w/v)		Lightness (L*), redness (a*), and yellowness (b*)	
		Before crosslink	After crosslink
20	L*	93.37 ± 2.15	85.05 ± 1.84
	a*	0.05 ± 0.11	-0.48 ± 0.05
	b*	-0.60 ± 0.23	7.26 ± 0.78
23	L*	96.79 ± 0.45	87.97 ± 0.30
	a*	0.17 ± 0.08	0.00 ± 0.08
	b	-0.49 ± 0.24	7.21 ± 0.06
26	L*	96.93 ± 0.12	91.44 ± 0.50
	a*	0.12 ± 0.03	-0.48 ± 0.04
	b	-0.32 ± 0.03	5.77 ± 0.19